J. Appl. Glycosci., **71**, 95−102 (2024)
doi:10.5458/jag.jag.JAG-2024_0003

Regular Paper

Construction of the Thermostable D-Allulose 3-Epimerase from *Arthrobacter globiformis* M30 by Protein Engineering Method

(Received February 27, 2024; Accepted May 18, 2024)
(J-STAGE Advance Published Date: October 29, 2024)

Kouhei Ohtani,[1,*] Kensaku Shimada,[1,*] Pushpa Kiran Gullapalli,[1] and Kazuhiko Ishikawa[1,†]

[1] *Matsutani Chemical Industry Co., Ltd.*
(*5−3 Kita-Itami, Itami 664−8508, Hyogo, Japan*)

Abstract: D-Allulose 3-epimerase catalyzes C-3 epimerization between D-fructose and D-allulose was found in *Arthrobacter globiformis* strain M30. The enzyme gene was cloned, and its recombinant enzyme and the mutant variants were expressed in *E. coli.* Using the information of the sequence and model structure, we succeed in the improvement of melting temperature for the enzyme without significant loss of the enzyme activity by protein engineering method. The melting temperatures were increased by 2.7, 2.1, 3.7, 5.1, and 8.0 ˚C for the mutants Glu75Pro, Arg137Lys, Ala200Lys, Ala270Lys, and Val237Ile, respectively. Each effect of the mutation was independent and additive. By integrating the above mutations, we constructed a thermostable mutant that exhibits a melting temperature 12 ˚C higher than wild type, and remains stable at 65 ˚C for 2 h. These highly stable properties suggest that the thermostable enzymes represent an ideal enzyme candidate for the industrial production of D-allulose.

Key words: rare sugar, isomerization, fructose, psicose, stability, crystal structure

INTRODUCTION

D-Allulose (or D-psicose) is a noncaloric sweetener which is a naturally occurring carbohydrate [1, 2] and recognized as a rare sugar, the physiological functions of which, such as moderating blood D-glucose levels and fat accumulation, are being focused on for human healthcare [3, 4]. D-Allulose has been accepted as Generally Recognized as Safe (GRAS; GRAS Notices 498 and others) by the US Food and Drug Administration (FDA). D-Allulose is attractive as a functional food ingredient. The enzyme for epimerization between D-fructose and D-allulose has been found as the ketose 3-epimerase [5]. The first crystal structure of the enzyme was determined for D-psicose 3-epimerase from *Agrobacterium tumefaciens* and deposited as pdb:2hk0 [6]. The enzyme is a tetramer and each monomer belongs to a TIM-barrel fold. The active site contains a metal ion with octahedral coordination to two water molecules and four residues that are absolutely conserved in the family. Structural evidence and site-directed mutagenesis experiment suggest that the metal ion plays an important role in catalysis by anchoring the bound D-fructose, and the conserved Glu150 and Glu244 carry out an epimerization reaction at the C-3 position. The substrate displaces water molecules in the active site, with a conformation mimicking the intermediate *cis*-enediolate [6]. It was reported that D-allulose 3-epimerase (one of the ketose 3-epimerases) from *Arthrobacter globiformis* strain M30 (AgDAE) can be used for the efficient production of D-allulose from D-fructose [5]. Recently, Matsutani Chemical Industry Co., Ltd. (Hyogo, Japan) has commercialized D-allulose (brand name: Astraea) using the enzyme. The cost is significantly affected by the thermostability of the enzyme and the enzymes with higher thermostability have been desired. Therefore, we tried to construct the thermostable mutants of AgDAE in this study.

The random approaches like error prone PCR or physical techniques to improve the thermostability of enzymes have been performed frequently. The rational design for thermostable enzymes without decreasing the specific activity is a goal for basic research as well as for industrial applications. However, commonly accepted and widely used strategy for efficient engineering is not known. Recently computational methods for the construction of thermostable enzyme have been developing for example using FoldX [7] and Rosetta [8]. However, the question whether the prediction of mutation sites by FoldX is more accurate than random based approaches is addressed [7].

In this study, we tried to construct the thermostable enzyme by protein engineering method using the principles of protein structure. From the sequence homology, it has been predicted that the tertiary structure and active site of the enzyme are almost same in the family. Therefore, we obtained the chance to identify mutation sites that do not affect the enzyme activity. It has been reported that thermostabilities of the enzymes were improved by the introduction

* These two authors contributed equally to this work.
† Corresponding author (Tel. +81−720−771−2052, E-mail: kazuhiko-ishikawa@matsutani.co.jp, ORCID ID:0000-0001-9845-0461)
Abbreviations: DAE, D-Allulose 3-epimerase; AgDAE, D-allulose 3-epimerase from *Arthrobacter globiformis* strain M30; AtDAE, D-allulose 3-epimerase from *Agrobacterium tumefacience*; CcDAE, D-allulose 3-epimerase from *Clostridium cellulolyticum*; PcDAE, D-allulose 3-epimerase from *Pseudomonas cichorii*; MlDAE, D-allulose 3-epimerase from *Mesorhizobium loti*; WT, wild type.

of Pro [9], introduction of salt bridge [10−12], and improvement of molecular packing [13−16]. In this study, we tried to construct the thermostable mutant enzymes by protein engineering method with the similar strategy described above. The thermostabilities were evaluated by melting temperature, temperature dependence on the activity, and residual activity after heat treatment.

MATERIALS AND METHODS

Materials. D-Allulose (Astraea) was prepared by Matsutani Chemical Industry Co., Ltd. (Hyogo, Japan). Peptone (Nucel 581PW) and Yeast extract (BSP-B) were purchased from Oriental Yeast (Tokyo, Japan). Other chemicals were purchased from Nacalai Tesque Inc. (Kyoto, Japan). Protein purification column (Superdex™ 200 increase 10/300 GL) was purchased from Cytiva (Tokyo, Japan).

Enzyme assay. D-Allulose 3-epimerase (DAE) activity assay was performed by the method based on the quantitative analysis by determining the amount of D-fructose produced from D-allulose [5]. The reaction mixture contained 2 mM $MgSO_4$ and 100 mM D-allulose in 50 mM phosphate buffer (pH 8.0), to which an appropriate amount of diluted enzyme was added, with a final volume of 1.0 mL. The reaction mixture was incubated at 50 ˚C for 10 min and the reaction was stopped by adding 0.04 mL of 5 % HCl solution. The amount of D-fructose produced was determined by high performance liquid chromatography (HPLC) analysis system [5] equipped with MCI GEL CK08EC column from Mitsubishi Chemical (Tokyo Japan) and RI detector. The injection volume was 10 μL, the distilled water was used as the mobile phase at flow rate of 0.4 mL/min, and the column temperature was kept at 80 ˚C. One unit of enzyme activity was defined as the amount of enzyme that could epimerize 1 μmol of the substrate per min. The values of k_{cat} and K_m for the substrates were determined by the least-square's method [17] for Michaelis-Menten equation at 50 ˚C in 50 mM sodium phosphate buffer (pH 8.0) containing 2 mM $MgSO_4$. For the reverse reaction activity (D-fructose→D-allulose), D-allulose produced was also determined by HPLC with the same method described above. Protein concentrations were determined using the Bradford protein assay kit (Bio-Rad Laboratories, Inc., Berkeley, CA, USA) with bovine serum albumin as the standard protein.

Enzyme preparation and purification. The structural gene encoding AgDAE [5] was constructed by PCR. The constructed structural gene of AgDAE amplified by PCR was fused with NcoI digested pQE60 using an In-Fusion HD Cloning Kit (Takara Bio Inc., Shiga, Japan). Using the plasmid, the transformant *E. coli* M15 was prepared and the recombinant enzyme of AgDAE was expressed. *E. coli* harboring the recombinant AgDAE was cultivated at 37 ˚C for 6 h in SB medium (3.2 % Peptone Nucel 581PW, 2.0 % Yeast extract BSP-B, and 0.5 % NaCl) containing 0.01 % ampicillin and 0.005 % kanamycin. Enzyme expression was induced by the addition of IPTG to the medium, resulting in a final concentration of 0.1 mM IPTG and cultivation was continued at 20 ˚C for overnight. The cells were then harvested by centrifugation. The collected cells were suspended in 50 mM sodium phosphate buffer (pH 8.0) containing 2 mM $MgSO_4$ and disrupted by sonication for 15 min. The resulting solution was heated at 55 ˚C for 15 min, and cell debris was removed by centrifugation. DNA present in the cell free extract was removed by using Nucleic Acid Removal Kit (ProFoldin, Hudson, MA, USA). The supernatant was applied onto a purification column (Superdex™ 200 increase 10/300 GL column). The active fractions were pooled and used for the experiments. The purity and molecular weight of the sample was determined by SDS-PAGE. The protein sample was mixed with Invitrogen NuPAGE™ LDS Sample Buffer (4X) and NuPAGE™ Reducing Agent (10X) (Thermo Fisher Scientific Inc., Waltham, MA, USA) to adjust the final concentration to 0.2 mg/mL. After heating at 70 ˚C for 10 min, each 5 μL of the prepared solution was loaded onto the SDS gel, as reported previously [5]. All mutant genes were constructed by PCR using a PrimeSTAR Max DNA Polymerase (Takara Bio Inc., Shiga, Japan) and the recombinant mutant enzymes were also prepared and purified, as described above.

Thermostability of the enzymes. The activity at 70 ˚C of AgDAE decreased considerably compared with that at 50 ˚C. Thus, the ratio of activity in percent at 70 and 50 ˚C (T70/50: activity at 70 ˚C / activity at 50 ˚C) was used for the index of their thermostability. Thermostability of the mutant enzymes were also determined as the melting temperature value (T_m) using "Protein Thermal Shift" Dye Assay kit (TSA: Thermo Fisher Scientific Inc.) [13]. The individual mutant samples were dissolved in 50 mM sodium phosphate buffer (pH 8.0) containing 2 mM $MgSO_4$. Assay kit's dye binds to exposed internal hydrophobic amino acid residues of the enzyme to monitor the thermal stability of proteins using a real-time PCR (Applied Biosystems Inc., Foster City, CA, USA). Measurement was performed according to the PCR System analysis software and assay kit user manual. The residual activity assay of the enzyme was performed by the method based on the quantitative analysis by determining the amount of D-fructose produced from D-allulose at 50 ˚C and pH 8.0 described above after the incubation at 65 and 70 ˚C.

RESULTS AND DISCUSSION

Preparation of the recombinant AgDAE.

The recombinant AgDAE was prepared and purified as described in Materials and Methods. The recombinant enzyme expression exceeding 0.2 mg per 1 mL (broth) was observed. After purification, the purified recombinant enzyme showed a single protein band with a molecular weight of about 32 kDa on SDS–PAGE (Fig. 1). The molecular mass of the purified enzyme was estimated as 130 kDa by the above gel filtration chromatography (data not shown). These results indicate that the recombinant AgDAE is a tetramer structure with four identical subunits as observed on native AgDAE [5]. Same results were observed for the mutant derivatives (Fig. 1). The individual enzyme solutions dialyzed against 50 mM sodium phosphate buffer (pH 8.0) containing 2 mM $MgSO_4$ were used for the following experiments.

Design of the thermostable mutants for AgDAE.

Sequence alignment of DAEs; *Agrobacterium tumefacience* (AtDAE; GenBank accession no: AAL45544) [18], *Clostridium cellulolyticum* (CcDAE; GenBank accession no: ACL75304), *Pseudomonas cichorii* (PcDAE; GenBank accession no: BAA24429), AgDAE [5], and *Mesorhizobium loti* (MlDAE; GenBank accession no: BAB50266) are

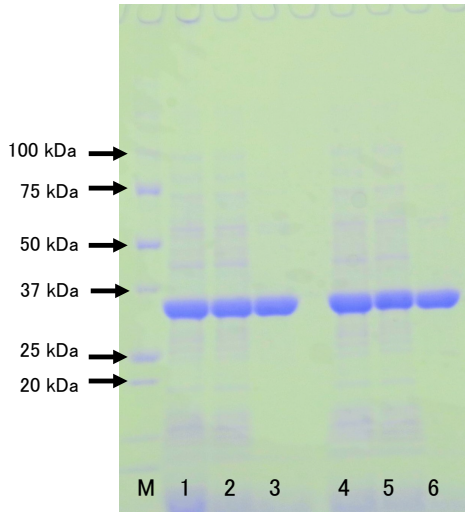

Fig. 1. SDS-PAGE of the purified wild type AgDAE (WT) and its mutants.

M: protein molecular-weight markers; lane 1, WT; lane 2, E75P; lane 3, S137K; lane 4, A200K; lane 5, V237I; lane 6, A270K. The prepared protein samples (0.2 mg/mL) and a molecular-weight markers (Precision plus protein pre stained standards: Bio-Rad Laboratory, Inc., Berkeley, CA, USA) were loaded into the wells of the gel.

shown in Fig. 2. The first crystal structure of DAE was determined as AtDAE and deposited (pdb:2hk0) [6]. The tertiary structural model of AgDAE constructed by AlphaFold2 (AF2) [19] exhibited high homology to that of AtDAE [6]. From the structural similarity, it was also clarified that the catalytic residues coordinating Mn^{2+} (Glu146, Asp179, His205, and Glu240) of AgDAE are well conserved in DAEs.

For the construction of the thermostable enzymes using protein engineering method, random mutagenesis and rational design mutagenesis approaches can be applied. If the high-throughput screening method for the enzyme is available, random mutagenesis approach can be employed for the construction of thermostable enzymes. For AgDAE, the enzyme assay is carried out by HPLC analysis. Therefore, it is difficult to use the random mutagenesis approaches for our research purposes. In this study, we tried to construct the thermostable mutant enzymes by the rational design. Using the information of the sequence alignment of DAE, thermostable AgDAE mutants are designed by sequence shuffling method of rational designed mutagenesis [13].

Proline is the only amino acid with a secondary amine, in that the side chain is directly connected to nitrogen of the main chain, preventing the rotation of phi angles of the peptide bond. Therefore, proline residues in proteins make the main chain at loop regions rigid and enhance the stability of enzyme. Furthermore, it has been proposed that the proline which introduced at loop regions decreases the configurational entropy of unfolding [9]. So far thermostable enzyme mutants have been constructed by the introduction of Pro residues [14−16]. From the sequence alignment and the structural information constructed by AF2, Pro77 of AgDAE is not conserved for DAEs (Fig. 2) and located at N-cap region of α-helix structure of contributing stability of the enzyme (Fig. 3) [20]. Furthermore, stable Asx-Pro-turn structure is identified at the position as Asp76-Pro77 (Fig. 3) contributing the stability with the related hydrogen bonds [21]. The preceding loop region is located at the surface of the enzymes (Fig. 3), and not conserved in the sequence (Fig. 2). In PcDAE, however, Pro is observed at the position corresponding residue to Glu75 in AgDAE (Fig. 2). Using the information of the model structure by AF2, it is suggested that Glu75 located at the loop region preceding the long α-helix structure (Fig. 2) is present on the surface of the enzyme and can be mutated to Pro without significantly steric hindrance (E75P: green in Fig. 3). Therefore, we would like to stabilize the loop region by the introduction of Pro with the characteristics mentioned above at the site. E75P mutation was employed.

From the sequence homology (Fig. 2) and the structural model of AgDAE by AF2 it is clarified that Val237 is conserved partially and located inside of the enzyme molecule (Fig. 4). In the sequence of PcDAE, Ile243 was observed at the corresponding position of Val237 in AgDAE (Fig. 2). Furthermore, its hydrophobic structural core observed around Val237 is constructed by hydrophobic residues (Met1, Val204, Ile206, Val228, leu276, and Leu280) (Fig. 4). The enough space for the substitution with Ile at that position of Val235 is observed. Therefore, it is estimated that Ile can be substitute for Val237 (V237I: green in Fig. 4) in AgDAE and the thermostability of the enzyme could be expected to be improved by the hydrophobic packing effect.

It has been reported that salt bridges play an important role in the thermostability of many proteins [22−24]. The ionizable side chains frequently form ion pairs in many protein structures. Since electrostatic attraction between opposite charges is strong *per se*, and long-range, salt bridges can be regarded as an important factor stabilizing the protein structure. In addition, many salt bridges involving Lys and Arg were observed at the surface of thermophilic enzymes [10–12, 25]. Introduction of Lys residue at the surface of the enzyme is one of the convenient methods for providing salt bridges. From the information of the sequence alignment (Fig. 2) and structural model of AgDAE, Ser137, Ala200, and Ala270 are present on the surface of the enzyme and can be selected as Lys substitution sites. Ser137 is located near Asp134 and Asp138 at C-terminus of α-helix structure on the surface of the enzyme molecule (Fig. 5A). In MlDAE, Lys is located at the position corresponding to Ser137 in AgDAE (Fig. 2). Ser137 in AgDAE can be mutated to Lys (S137K) without steric hindrance and the salt bridges among Asp134, Asp138, and Lys137 are expected (Fig. 5A). Ala200 is located at loop region near Glu167 and Glu199 on the surface of AgDAE (Fig. 5B). In PcDAE, Lys is located at the position corresponding to Ala200 in AgDAE (Fig. 2). Ala200 in AgDAE can be mutated to Lys (A200K) and the salt bridges among Glu167, Glu199, and Lys200 are expected (Fig. 5B). Ala270 was located at C-terminal α-helix structure and related to the association between two molecules in the tetramer structure of AgDAE. Around Ala270, many acidic residues (Asp264, Asp278, Glu28, Glu266, and Glu267) are observed (Fig. 5C). In MlDAE, Lys is located at the position corresponding to Ala270 in AgDAE (Fig. 2). We cannot speculate the detailed information for the expected salt bridges. However, it can be estimated that A270K mutant forms some salt bridges among them (Fig. 5C). Therefore, S137K, A200K, and A270K mutants were employed.

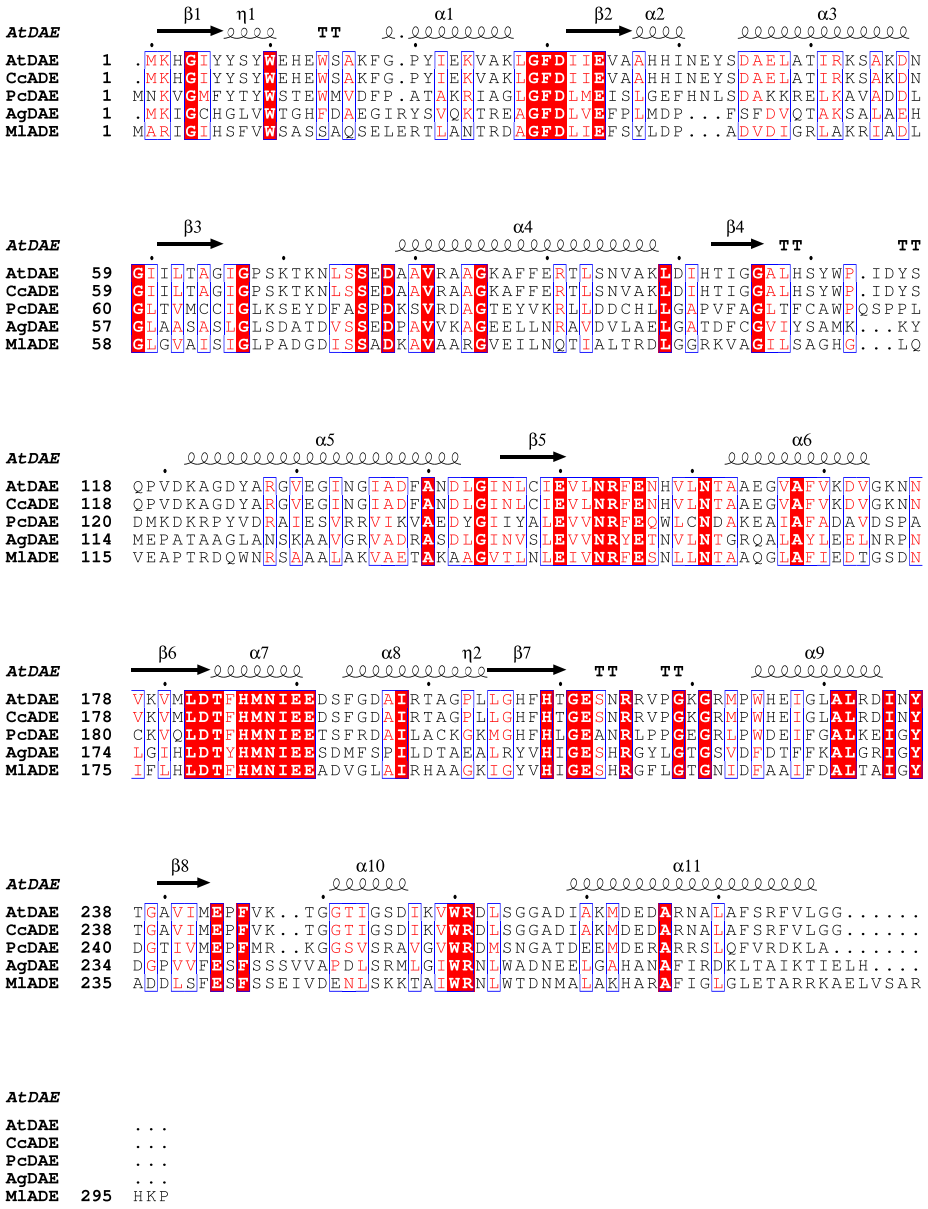

Fig. 2. Multiple sequence alignment of DAE and its homologs.

The sequences for DAE from *A. globiformis* strain M30 (AgDAE; GenBank accession no: AB981957) [5] were aligned with those from *A. tumefacience* (AtDAE; GenBank accession no: AAL45544), *C. cellulolyticum* (CcDAE; GenBank accession no: ACL75304), *P. cichorii* (PcDAE; GenBank accession no: BAA24429), and *Mesorhizobium loti* (MlDAE; GenBank accession no: BAB50266). The residues in red enclosed in a blue box are highly conserved and those with red background are identical. The secondary structure elements are shown by the crystal structural information of AtDAE [6].

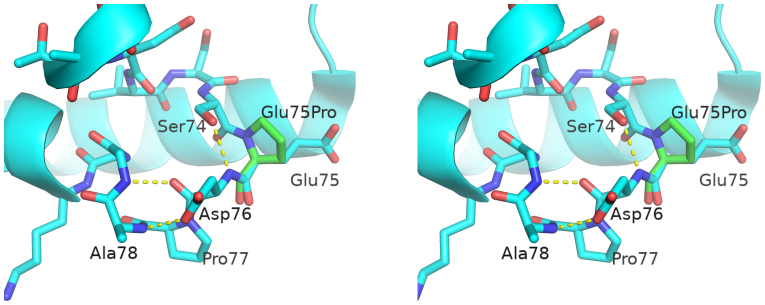

Fig. 3. Cross-eyed stereo figures of the model structure of the loop region (Glu75-Asp76-Pro77-Ala78) of AgDAE by AF2.

Ser74, Asp76, Pro77, Ala78 which relate to hydrogen bonds are shown with dashed lines in the cyan stick models on the loop region. Mutation site for Glu75Pro is shown in green.

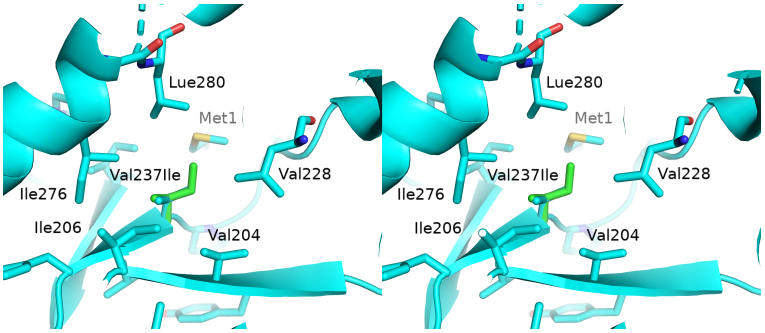

Fig. 4. Cross-eyed stereo figures of the structure of the hydrophobic region around Val237 by AF2.
Mutation site for Val237Ile is shown in green.

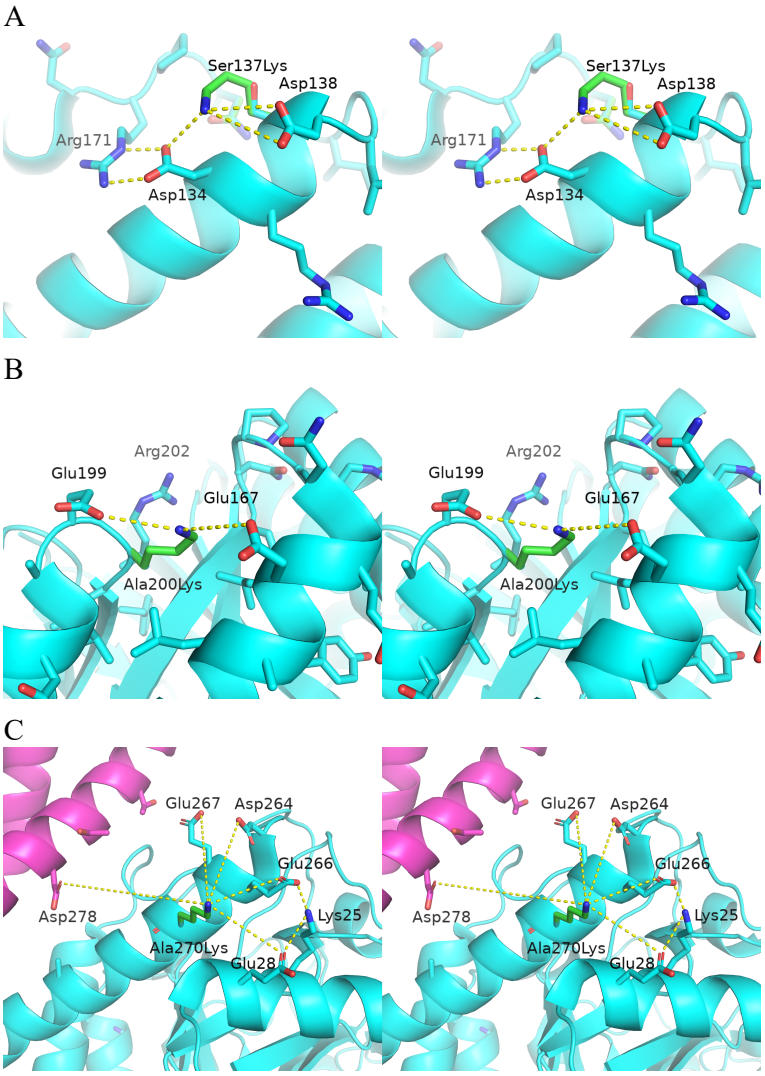

Fig. 5. Cross-eyed stereo figures of the structure of speculated salt bridge sites by AF2 around Ser137 (A), Ala200 (B), and Ala270 (C) by mutation of Lys.
Mutation sites of Ser137Lys (A), Ala200Lys (B), and Ala270Lys (C) and speculated salt bridges are shown in green stick model and dashed lines, respectively. Another molecule in the tetramer structure of AgDAE is shown in magenta (C).

Construction and comparison of the thermostable mutants.

Recombinant AgDAE and each mutant described above were expressed well. All enzymes were prepared and purified (Fig. 1). The enzymatic activity assays were performed as described previously [5]. Their specific activities at 50 ˚C were not affected by these mutations significantly (Table 1). The activity at 70 ˚C of wild type AgDAE (WT) decreased considerably compared with that at 50 ˚C. Thus, the ratio of activity in percent at 70 and 50 ˚C (T70/50: activity at 70 ˚C / activity at 50 ˚C) was used for the index of their thermostability. Table 1 shows the activity ratio in percent for the mutants. All mutant derivatives exhibit higher thermostability than WT. To evaluate the thermostability of the mutants directly, the value of T_m was also examined. All mutants exhibit higher T_m than that of WT (Table 1). These results show that all positions for these mutations are ideal positions for the

Table 1. Characteristics of AgDAE and the mutants.

	Specific activity (U/mg)	Relative activity (%)	T70/50	T_m (°C)
WT	93.0 ± 9	100	0.70	66.6
E75P	106 ± 11	114	0.84	69.3
S137K	115 ± 11	124	0.92	68.7
A200K	99.5 ± 5	107	1.0	70.3
V237I	90.2 ± 10	97.5	1.66	74.6
A270K	113 ± 23	122	1.46	71.7
MT5	76.3 ± 15	82.0	2.04	78.9

The enzyme activities were measured at 50 °C in 50 mM sodium phosphate buffer (pH 8.0) containing 2 mM $MgSO_4$. The unit was determined in triplicate with the standard deviation. Relative activity was set to 100 % with WT as the reference. The ratio of the activities (T70/50: (activity at 70 °C)/(activity at 50 °C)) was also measure in 50 mM sodium phosphate buffer (pH 8.0) containing 2 mM $MgSO_4$. The values of T_m (°C) were measured by TSA.

Table 2. Comparison of kinetic parameters between WT and MT5.

Allulose→Fructose	K_m (mM)	k_{cat} (min^{-1})	k_{cat}/K_m ($min^{-1}.mM^{-1}$)
WT	11.7 ± 0.7	(2.63 ± 0.03) × 10^3	(2.25 ± 0.14) × 10^2
MT5	15.7 ± 1.4	(2.33 ± 0.04) × 10^3	(1.01 ± 0.09) × 10^2
Fructose→Allulose	**K_m (mM)**	**k_{cat} (min^{-1})**	**k_{cat}/K_m ($min^{-1}.mM^{-1}$)**
WT	21.1 ± 5.6	(1.92 ± 0.11) × 10^3	(0.91 ± 0.25) × 10^2
MT5	27.8 ± 7.2	(1.59 ± 0.10) × 10^3	(0.57 ± 0.09) × 10^2
k_{cat}/K_m (Allulose→Fructose) / k_{cat}/K_m (Fructose→Allulose)			
WT	2.47 ± 0.69		
MT5	1.76 ± 0.33		

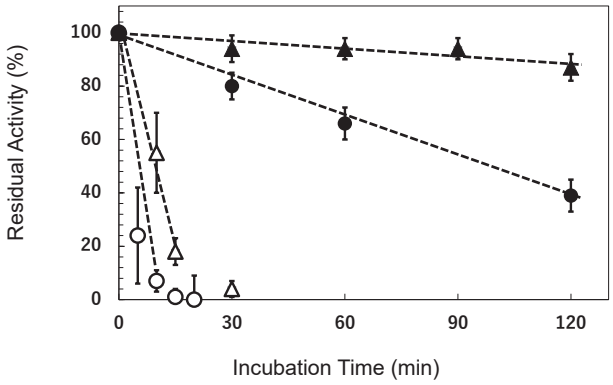

Fig. 6. Residual activities of WT and M5 after heating.
Enzyme samples (0.5 mg/mL) in a 50 mM sodium phosphate buffer (pH 8.0) containing 2 mM $MgSO_4$ were incubated at 65 °C (△: WT and ▲: MT5) and 70 °C (○: WT and ●: MT5) for each period. After the heat treatment, the residual activities were measured at 50 °C for 10 min in the same buffer described above. The standard deviation of three replicates was indicated by error bars.

construction of thermostable enzymes.

To examine the significant positive effects of the mutants on the enzyme's thermostability, we prepared the integrated mutant (MT5: E75P/S137K/A200K/V237I/A270K) and characterized the functions. The overall structural model of MT5 predicted by AF2 was almost same as that of WT. Furthermore, it can be speculated that the 5 mutation sites do not interact with each other in the tertiary structure. Table 1 shows that MT5 does not influence the specific activity significantly and their individual effect for thermostability caused by mutations was independent and additive (non-quantitatively). By integrating the above mutations, we constructed a thermostable mutant (MT5) that exhibits a melting temperature 12 °C higher than WT. For the optimum temperature of the enzyme, the detailed data is not shown. However, the data of T70/50 (Table 1) shows that the temperature dependence on the activity and thermostability of MT5 are improved. The residual activities of the enzymes (WT and MT5) were examined after the incubation at 65−70 °C and pH 8.0. The data of the residual activity exhibits the irreversible inactivation after the heat treatment. Therefore, the data indicate the thermostability of the enzyme including the effect of the protein refolding process after the heat treatment. As shown in Fig. 6, WT lost its activity after incubation at 65 °C for 20 min. However, MT5 does not lose significant activities even after 120 min incubation at 65 °C. It was clarified that thermostable MT5 exhibited highly positive effects for the residual activity assay. The date for the individual mutants (E75P, S137K, A200K, V237I, and A270K) also showed the positive effects for the residual activity assay between WT and MT5 (data not shown).

The characteristics of MT5 were examined at 50 °C. Enzyme kinetics were investigated with either D-allulose and D-fructose as the substrates at 50 °C in 50 mM sodium phosphate buffer (pH 8.0) containing 2 mM $MgSO_4$ (Table 2). The values of K_m for the both substrates were slightly increased by the mutation. However, the significant difference for the values of k_{cat} for the both substrates between WT and MT5 was not observed (higher than 82 % of WT). In addition, the values of k_{cat}/K_m(Allulose→Fructose) / k_{cat}/K_m(Fructose→Allulose) for WT and MT5 fall roughly within the range specified by a rule of Haldane equation [26] [k_{cat}/K_m(Allulose→Fructose) / k_{cat}/K_m(Fructose→Allulose) = K (equilibrium constant for Fructose/Allulose)] (Table 2). The above results indicate that all mutants and MT5 prepared are thermostabilized and can be used for industrial application.

In this study, we obtained several thermostable mutants without depressing specific activity. The obtained thermostable mutants exhibit high optimum and melting temperature, and can be used for industrial scale applications. The sequence and tertiary-structural information which lead to the thermostable mutant enzyme design provides a method applicable for other enzymes. The effect by the introduction of the

individual salt bridge in enzyme protein is not relatively high. However, we can succeed in improving the enzyme thermostability by introducing of Lys at the surface of the enzyme molecule. Furthermore, many salt bridges involving Lys and Arg have been observed at the surface of thermophilic enzymes [10−12, 25]. By their additive effects, thermostable mutants can be constructed easily. Increasing the effect of hydrophobic interaction inside the enzyme protein provides the high effect for the thermostability (Table 1). Substitution of Ile for Val indicates the increase of the methyl residue volume in the protein molecule. Using the tertiary structural and sequence information, we will be able to find the suitable position of which Val can be changed to Ile without steric hindrance. In a similar way, the thermostability of the enzymes might be also improved by the substitution of Thr for Ser. However, we have to pay careful attention that the enhancement of hydrophobic interactions and the steric hindrance by the mutation are double-edged sword. Thermostabilization is an important tool for industrial applications, not only for DAE but also for other enzymes. In this study, we described how the thermostability of AgDAE was increased via several mutations. Using the information of the sequence homology among DAEs, we have a chance to thermostabilize the other DAEs by modify the positions corresponding to the five mutation sites described above. The sequence shuffling method we employed, helped us to obtain a thermostable DAE mutant without suppressing the specific activity. Sequence shuffling is not only a method to sort out mutant candidates, but also a method that sheds light on the difference between the structures of catalytically homologous enzymes derived from diverse species.

Additional mutations.

The experiment for the additional mutations was performed. For the introduction of Pro, the position of 21, 66, 214, and 220 are also proposed from the sequence alignment (Fig. 2). The mutants Y21P, L66P, L214P, and D220P are employed and examined. The mutant L66P was not expressed. This position exists within the interior of the enzyme molecule, potentially leading to steric hindrance and/or misfolding. The other mutants were expressed well. The values of T70/50 for Y21P, L214P, and D220P were 0.66, 0.71 and 0.73, respectively. Significant thermostability was not observed for the mutants. Additionally for the introduction of salt bridge and the hydrophobic interaction, the position of A95R, V91I, V105I, and V219I can be proposed from the sequence alignment (Fig. 2), and the mutants A95R, V91I, V105I, and V219I are employed and examined. These mutants were expressed well. The values of T70/50 for A95R, V91I, V105I, and V219I were 0.84, 0.85, 0.21, and 2.44, respectively. Improvement of thermostability was observed in some of the mutants. However, their specific activities were decreased. The trade-off relationship between enzyme activity and thermostability also needs to be taken into consideration. The detailed study for the effects of the additional mutations is in progress.

CONCLUSION

It is evident that the combination of these amino acid modifications resulted a mutant that is more resistant to thermal denaturation. Our approach created the enzyme with 12 ˚C higher thermostability than WT and the mutant enzyme maintained the residual activity at 65 ˚C for 120 min. The thermostability produced by intra-intermolecular interactions didn't affected the specific activity of the enzyme when compared WT. The generated thermostable enzyme offers the effective industrial application.

CONFLICTS OF INTEREST

Kouhei Ohtani, Kensaku Shimada, Pushpa Kiran Gullapalli, and Kazuhiko Ishikawa are employees of Matsutani Chemical Industry Co., Ltd.

ACKNOWLEDGMENTS

We thank Dr. Hiromi Yoshida of Life Science Research Center and Faculty of Medicine in Kagawa University (Kagawa, Japan) and her co-workers of Rare Sugar Research Center and Faculty of Agriculture of Kagawa University (Kagawa, Japan) for their kind help in verifying the questionable data related to the crystal structure of the enzymes.

We gratefully acknowledge the work of past and present members of our laboratory.

REFERENCES

[1] Matsuo T, Suzuki H, Hashiguchi M, Izumori K. D-psicose is a rare sugar that provides no energy to growing rats. J Nutr Sci Vitaminol (Tokyo). 2002; 48: 77−80.

[2] Iida T, Kishimoto Y, Yoshikawa Y, Hayashi N, Okuma K, Tohi M, et al. Acute D-psicose administration decreases the glycemic responses to an oral maltodextrin tolerance test in normal adults. J Nutr Sci Vitaminol (Tokyo). 2008; 54: 511−4.

[3] Hayashi N, Iida T, Yamada T, Okuma K, Takehara I, Yamamoto T, et al. Study on the postprandial blood glucose suppression effect of D-psicose in borderline diabetes and the safety of long-term ingestion by normal human subjects. Biosci Biotechnol Biochem. 2010; 74: 510−9.

[4] Chung YM, Hyun Lee J, Youl Kim D, Hwang SH, Hong YH, Kim SB, et al. Dietary D-psicose reduced visceral fat mass in high-fat diet-induced obese rats. J Food Sci. 2012; 77: H53−8.

[5] Yoshihara A, Kozakai T, Shintani T, Matsutani R, Ohtani K, Iida T, et al. Purification and characterization of D-allulose 3-epimerase derived from *Arthrobacter globiformis* M30, a GRAS microorganism. J Biosci Bioeng. 2017; 123: 170−6.

[6] Kim K, Kim HJ, Oh DK, Cha SS, Rhee S. Crystal structure of D-psicose 3-epimerase from *Agrobacterium tumefaciens* and its complex with true substrate D-fructose: a pivotal role of metal in catalysis, an active site for the non-phosphorylated substrate, and its conformational changes. J Mol Biol. 2006; 361: 920−31.

[7] Buss O, Rudat J, Ochsenreither K. FoldX as protein engineering tool: Better than random based approaches? Comput Struct Biotechnol J. 2018; 16: 25−33.

[8] Peccati F, Alunno-Rufini S, Jimenez-Oses G. Accurate prediction of enzyme thermostabilization with rosetta using AlphaFold ensembles. J Chem Inf Model. 2023; 63: 898−909.

[9] Matthews BW, Nicholson H, Becktel WJ. Enhanced protein thermostability from site-directed mutations that decrease the entropy of unfolding. Proc Nat Acad Sci. 1987; 84: 6663−7.

[10] Arnott MA, Michael RA, Thompson CR, Hough DW, Danson MJ. Thermostability and thermoactivity of citrate synthases from the thermophilic and hyperthermophilic archaea, *Thermoplasma acidophilum* and *Pyrococcus furiosus*. J Mol Biol. 2000; 304: 657−68.

[11] Christodoulou E, Rypniewski WR, Vorgias CR. High-resolution X-ray structure of the DNA-binding protein HU from the hyper-thermophilic *Thermotoga maritima* and the determinants of its thermostability. Extremophiles. 2003; 7: 111−22.

[12] Tanaka T, Sawano M, Ogasahara K, Sakaguchi Y, Bagautdinov B, Katoh E, et al. Hyper-thermostability of CutA1 protein, with a denaturation temperature of nearly 150 degrees C. FEBS Lett. 2006; 580: 4224−30.

[13] Nakabayashi M, Kamachi S, Malle D, Yanamoto T, Kishishita S, Fujii T, et al. Construction of thermostable cellobiohydrolase I from the fungus *Talaromyces cellulolyticus* by protein engineering. Protein Eng Des Sel. 2019; 32: 33−40.

[14] Ishikawa K, Kataoka M, Yanamoto T, Nakabayashi M, Watanabe M, Ishihara S, et al. Crystal structure of beta-galactosidase from *Bacillus circulans* ATCC 31382 (BgaD) and the construction of the thermophilic mutants. FEBS J. 2015; 282: 2540−52.

[15] Watanabe M, Fukada H, Ishikawa K. Construction of thermophilic xylanase and its structural analysis. Biochemistry. 2016; 55: 4399−409.

[16] Kozome D, Uechi K, Taira T, Fukada H, Kubota T, Ishikawa K. Structural analysis and construction of a thermostable antifungal chitinase. Appl Environ Microbiol. 2022; 88: e0065222.

[17] Sakoda M, Hiromi K. Determination of the best-fit values of kinetic parameters of the Michaelis-Menten equation by the method of least squares with the Taylor expansion. J Biochem. 1976; 80: 547−55.

[18] Kim HJ, Hyun EK, Kim YS, Lee YJ, Oh DK. Characterization of an *Agrobacterium tumefaciens* D-psicose 3-epimerase that converts D-fructose to D-psicose. Appl Environ Microbiol. 2006; 72: 981−5.

[19] Jumper J, Evans R, Pritzel A, Green T, Figurnov M, Ronneberger O, et al. Highly accurate protein structure prediction with AlphaFold. Nature. 2021; 596: 583−9.

[20] Viguera AR, Serrano L. Stable proline box motif at the N-terminal end of α-helices. Protein Sci. 1999; 8: 1733−42.

[21] Pinsker A, Einsiedel J, Harterich S, Waibel R, Gmeiner P. A highly efficient type I β-turn mimetic simulating an Asx-Pro-turn-like structure. Org Lett. 2011; 13: 3502−5.

[22] Makhatadze GI, Loladze VV, Ermolenko DN, Chen X, Thomas ST. Contribution of surface salt bridges to protein stability: guidelines for protein engineering. J Mol Biol. 2003; 327: 1135−48.

[23] Takano K, Tsuchimori K, Yamagata Y, Yutani K. Contribution of salt bridges near the surface of a protein to the conformational stability. Biochemistry. 2000; 39: 12375−81.

[24] Strop P, Mayo SL. Contribution of surface salt bridges to protein stability. Biochemistry. 2000; 39: 1251−5.

[25] Mine S, Nakabayashi M, Ishikawa K. Crystal structure of thermostable acetaldehyde dehydrogenase from the hyperthermophilic archaeon *Sulfolobus tokodaii*. Acta Crystallogr F Struct Biol Commun. 2023; 79: 159−65.

[26] Briggs GE, Haldane JB. A note on the kinetics of enzyme action. Biochem J. 1925; 19: 338−9.